

High Rate Capability Achieved by Reducing the Miscibility Gap of $\text{Na}_{4-x}\text{MnV}(\text{PO}_4)_3$

Ao Tang^a, Weiguang Lin^b, Dongdong Xiao^b, Chaoqun Shang^a, Min Yan^a, Zhanhui Zhang^a, Katerina Aifantis^c, Pu Hu^{a*}

^a Hubei Key Laboratory of Plasma Chemistry and Advanced Materials, School of Materials Science and Engineering, Wuhan Institute of Technology, Wuhan, 430205, China

^b Huairou Division, Institute of Physics, Chinese Academy of Sciences, Beijing 101400, P. R. China

^c Department of Mechanical and Aerospace Engineering, University of Florida, Gainesville, Florida 32603, United States

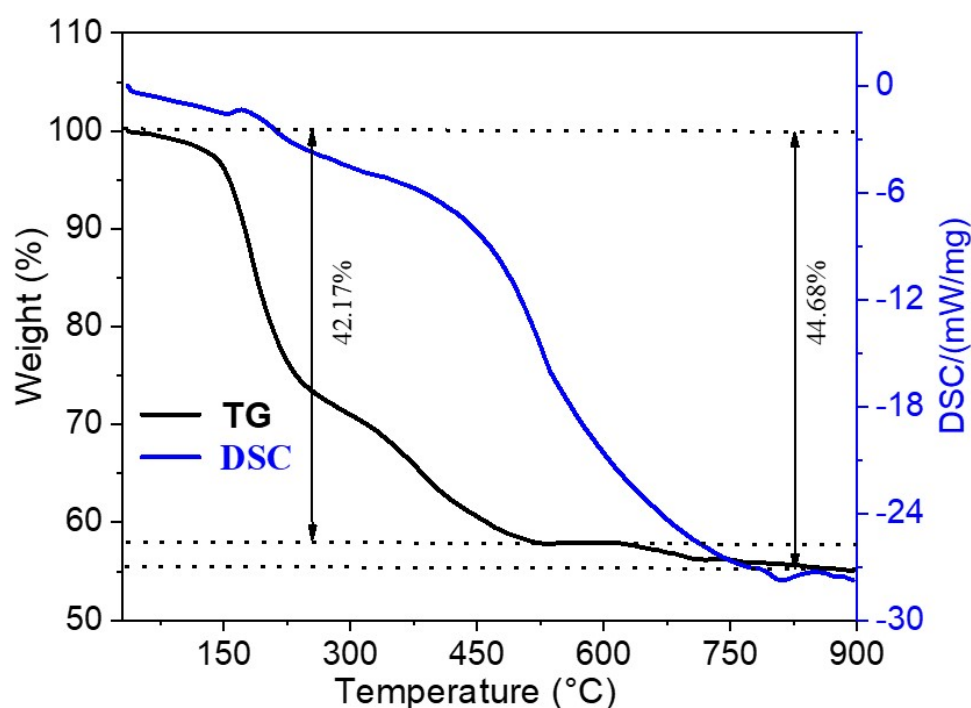


Figure S1 TG-DSC curves for heat treatment of NMVP precursors in argon.

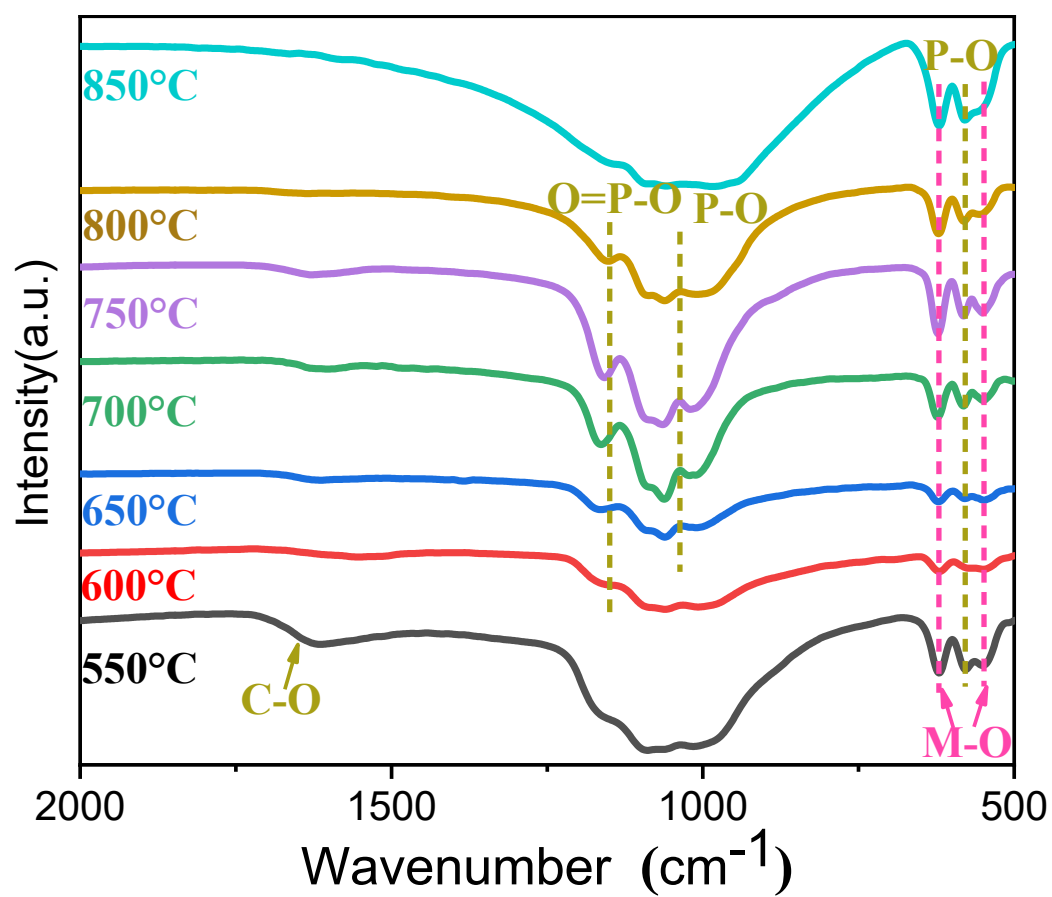


Figure S2 The FTIR spectra of NMVP materials at different temperatures.

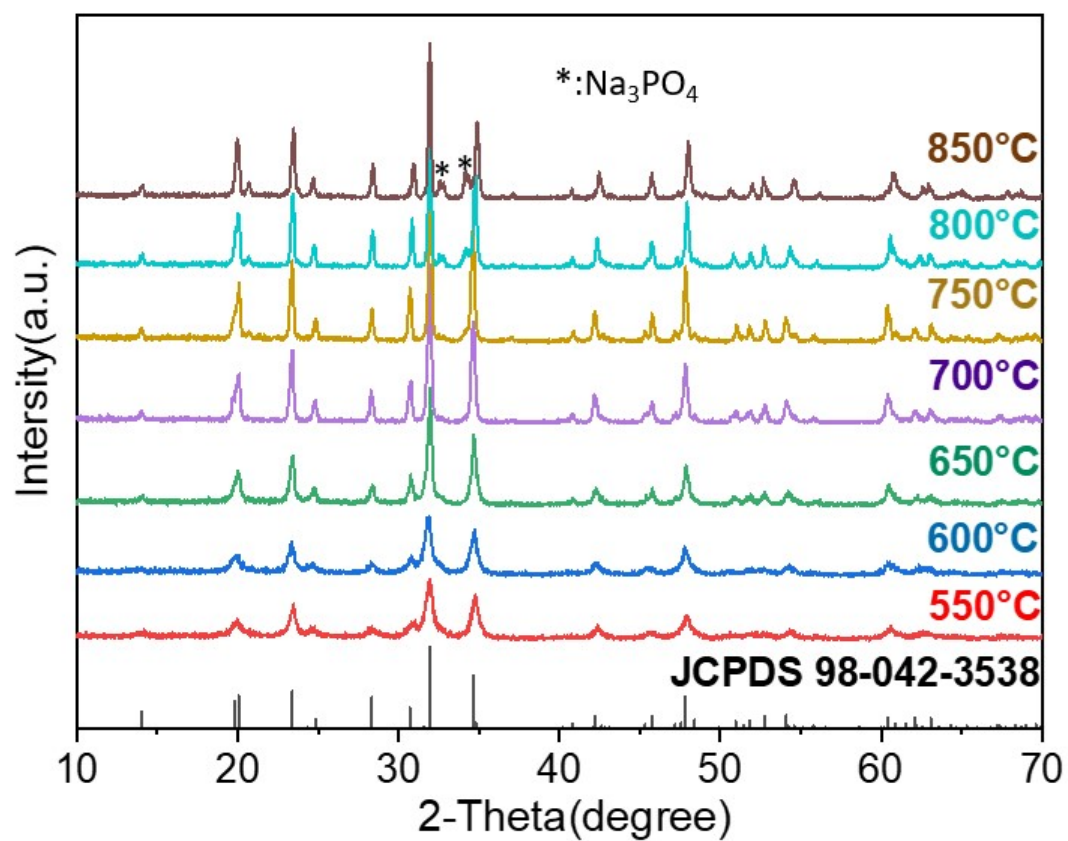


Figure S3 The XRD of NMVP materials at different temperatures.

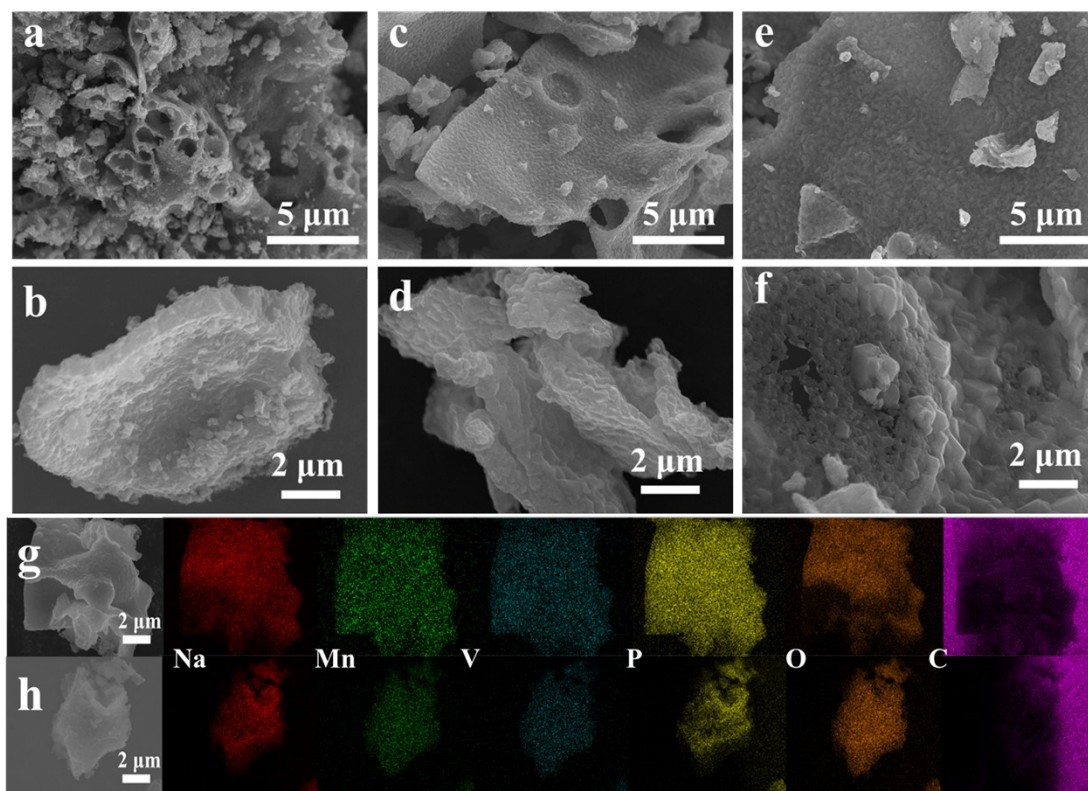


Figure S4 The SEM images of (a,b)NMVP-600, (c,d) NMVP-650 and (e,f) NMVP-700, and SEM image of NMVP-750 (g,h) with the corresponding elemental mappings of NMVP-600 and NMVP-700.

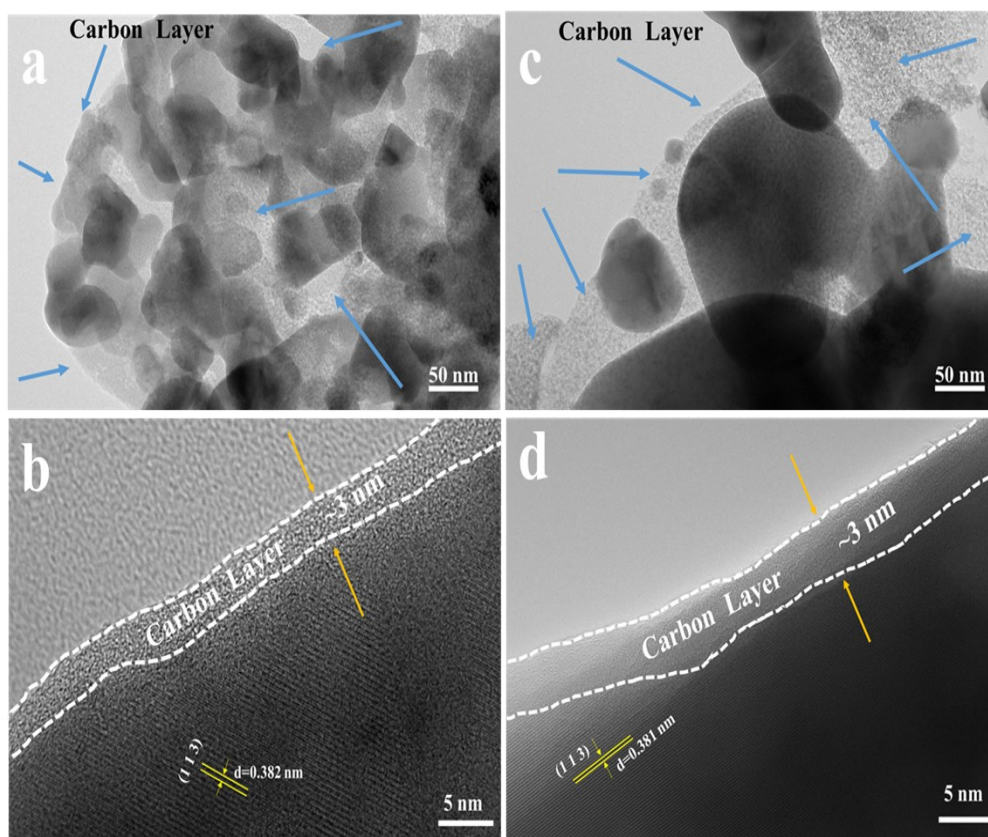


Figure S5 TEM images with different magnifications and coated carbon layer length NVMP-600 (a, b) and NVMP-700 (c, d).

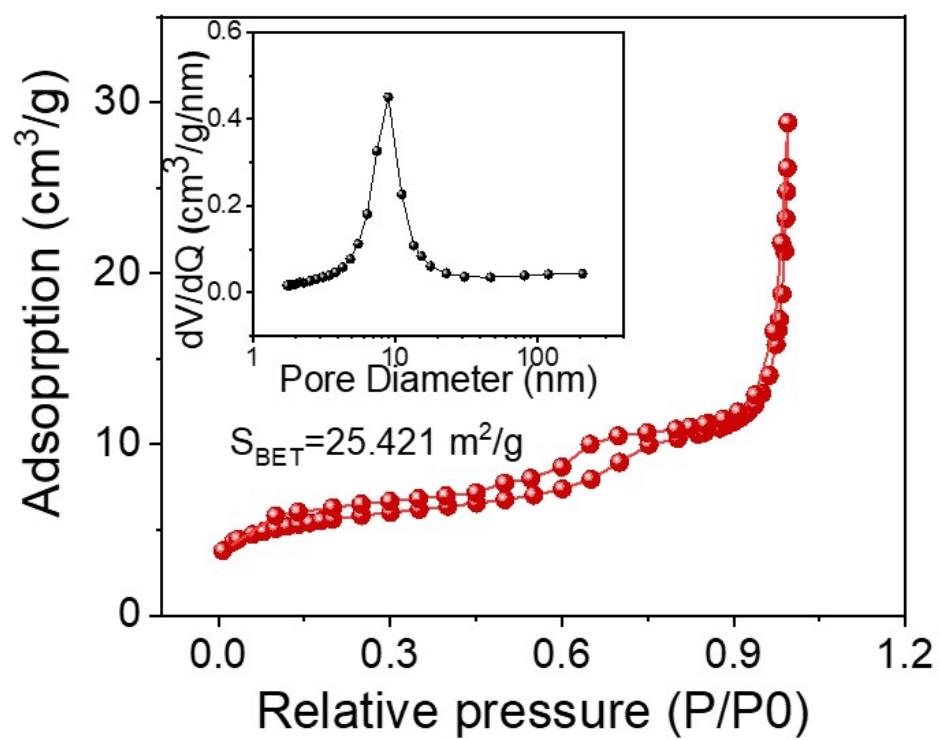


Figure S6 The nitrogen adsorption-desorption curves with inserted pore-size distribution of NVMP-700

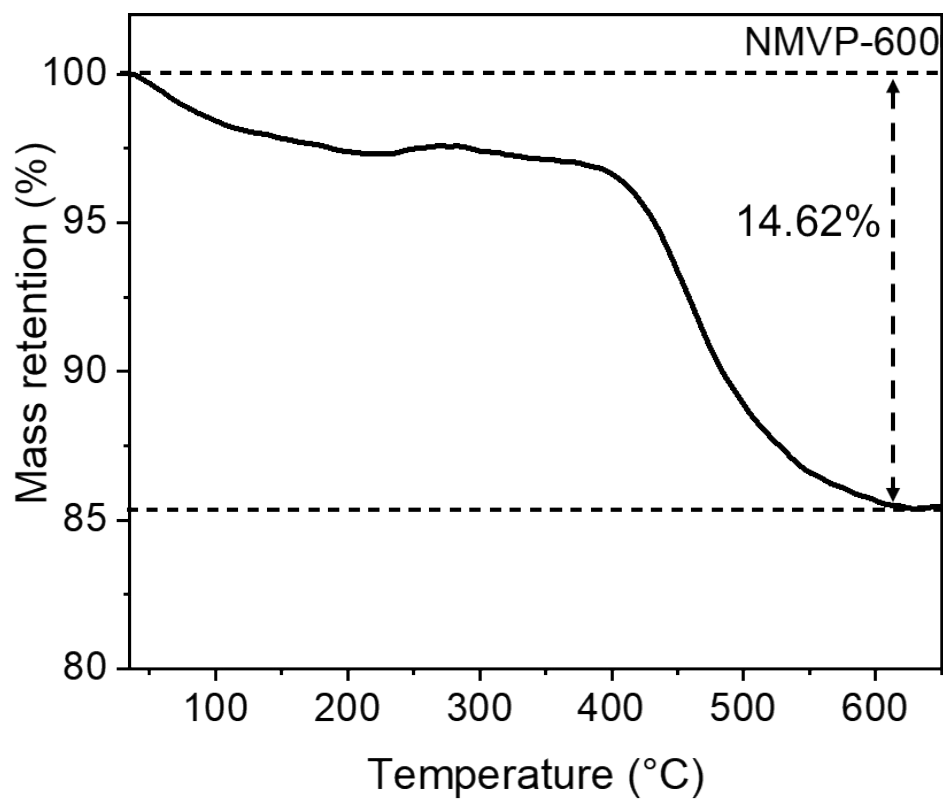


Figure S7 Thermogravimetry curves of NVMP-600 and NMVP-700 samples.

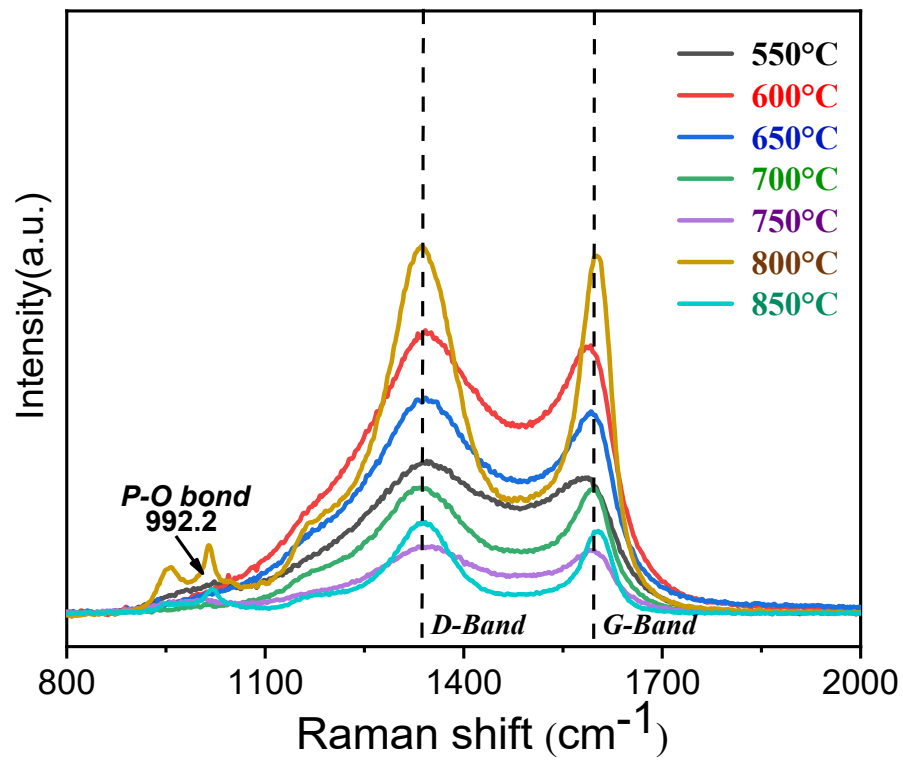


Figure S8 The Raman spectrum comparison of NMVP materials at different temperatures.

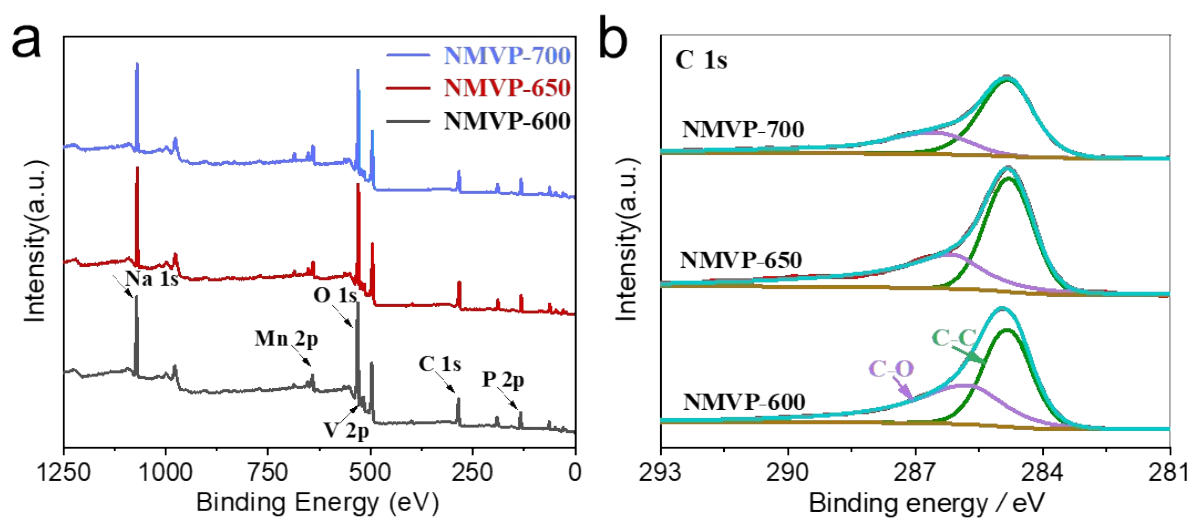


Figure S9 The XPS spectra of (a) whole spectrum and (b) C 1s.

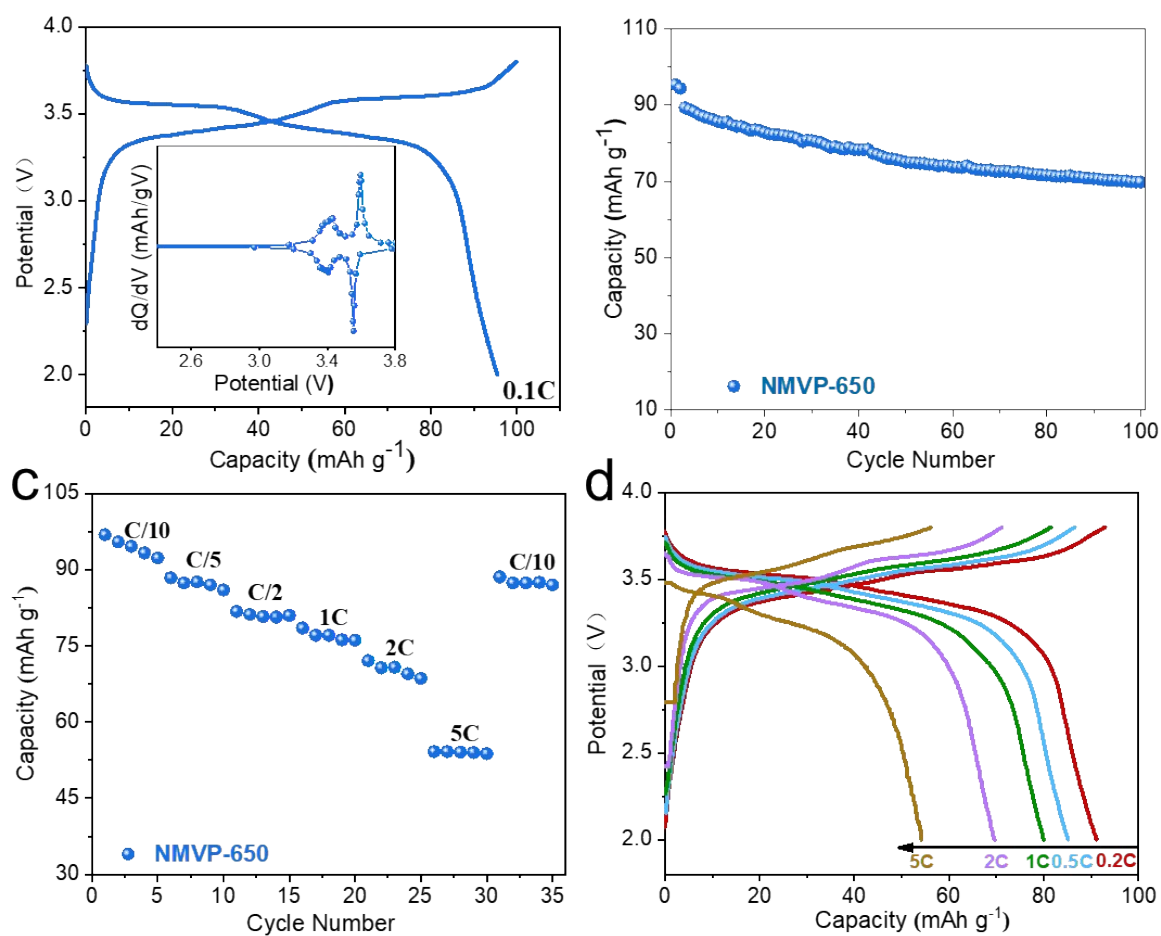


Figure S10 NMVP-650 cathodes (a) The initial charge/discharge curve, (b) Cycle performance, (c) Rate capability, (d) The charge/discharge curves at various current densities

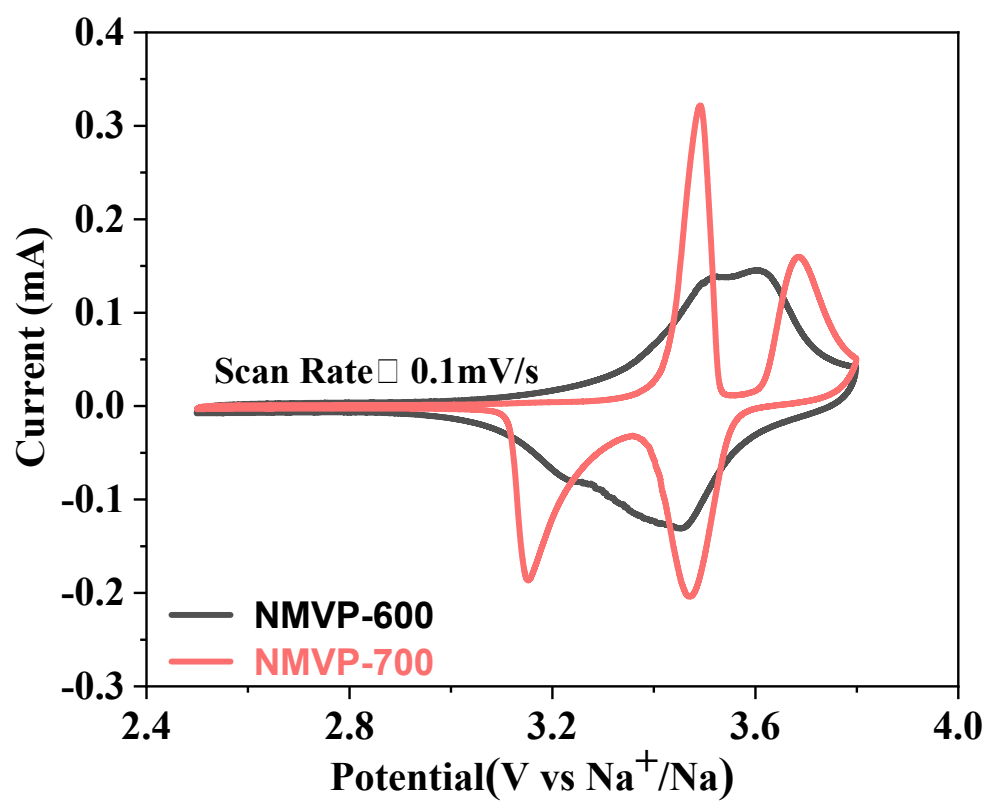


Figure S11 CV curves of NMVP-600 and NMVP-700 cathode at 0.1mV;

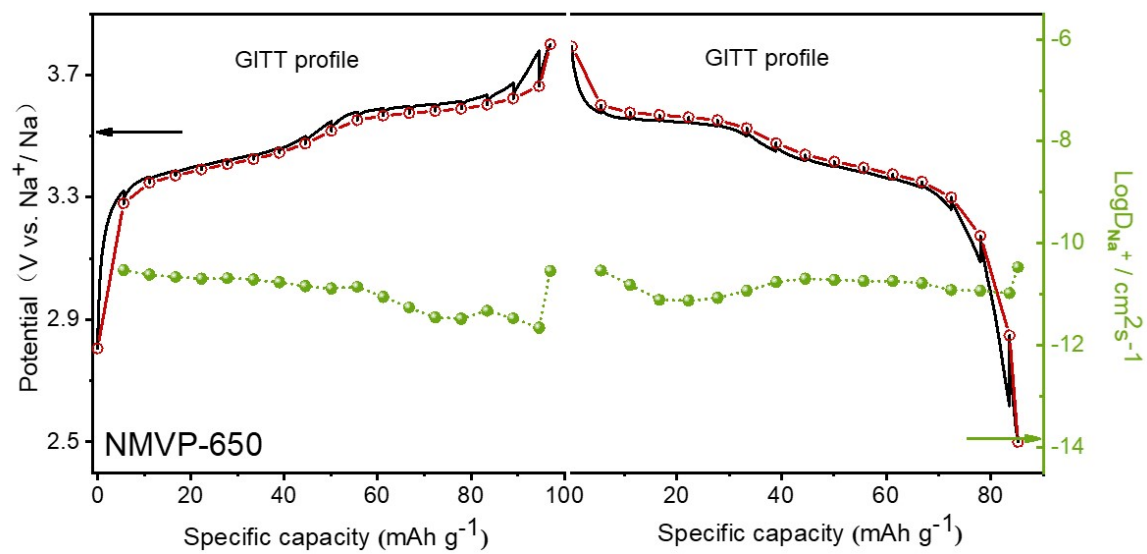


Figure S12 GITT curves and profiles of Na-ion chemical diffusion coefficient of NMVP-650